# Supplementary Information

## Semiconductor $TiO_2$ Thin Film Electrolyte Fuel Cell

Wenjing Dong[1], Yuzhu Tong[1], Bin Zhu[1,2,3*], Haibo Xiao[1], Lili Wei[1], Chao Huang[1], Baoyuan Wang[1], Xunying Wang[1], Jung-Sik Kim[3], Hao Wang[1*]

[1]Key Laboratory of Ferro & Piezoelectric Materials and Devices of Hubei Province, Faculty of Physics and Electronic Science, Hubei University, Wuhan, Hubei 430062, P. R. China

[2] Faculty of Materials Science and Chemistry, China University of Geosciences, 388 Lumo Road, Wuhan 430074, China

[3]Department of Aero & Auto Engineering, Loughborough University, Ashby Road, Loughborough, UK, LE11 3TU

*Corresponding author:* binzhu@kth.se (B. Z.), wangh@hubu.edu.cn (H.W.)

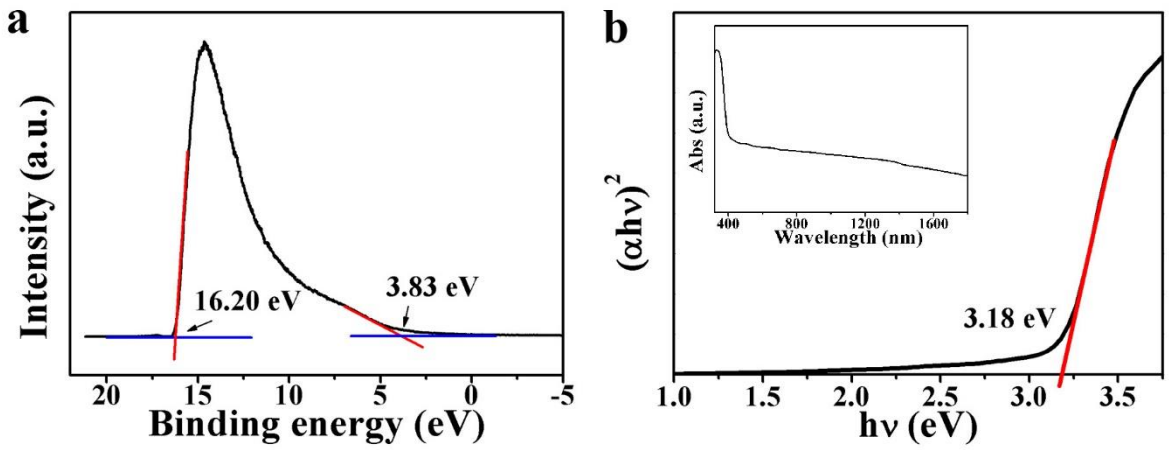


**Fig. S1** UPS (a) and optical band gap (b) study of Sm doped $CeO_2$.

The energy band level of Sm doped $CeO_2$ (SDC) was extracted from Ultraviolet Photoelectron Spectroscopy (UPS) and absorption spectroscopy. From UPS study, the valance band level was at -8.83 eV (=-[21.2-(16.20-3.83)] eV) below the vacuum energy level. As the optical band gap of SDC was measured to be 3.18 eV from absorption spectroscopy, the conduction band level was calculated to be at -5.65 eV (=-8.83+3.18 eV) below the vacuum energy level, which is much lower than the redox potential of $H_2/H^+$ (- 4.5 eV).

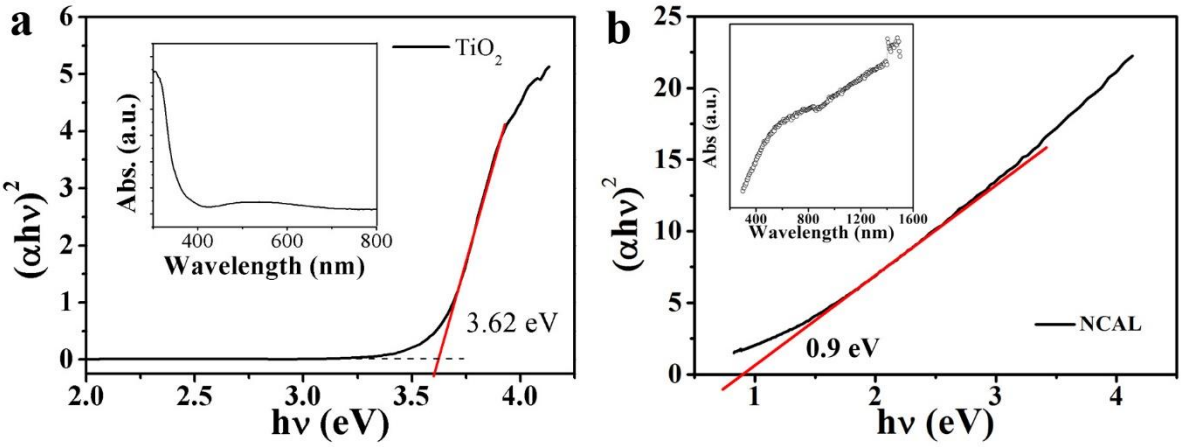


**Fig. S2** Tauc plots and UV-Vis-Infrared absorption spectra of (a) $TiO_2$ and (b) NCAL.

The UV-Vis-Infrared absorption spectroscopy was measured on UV3600 (SHIMADZU) equipped

with an integrating sphere. The NCAL powders were dispersed in alcohol during the test while the $TiO_2$ thin film was prepared on glass substrate. The optical energy band gap for $TiO_2$ and NCAL is calculated to be 3.62 eV and 0.9 eV, respectively.

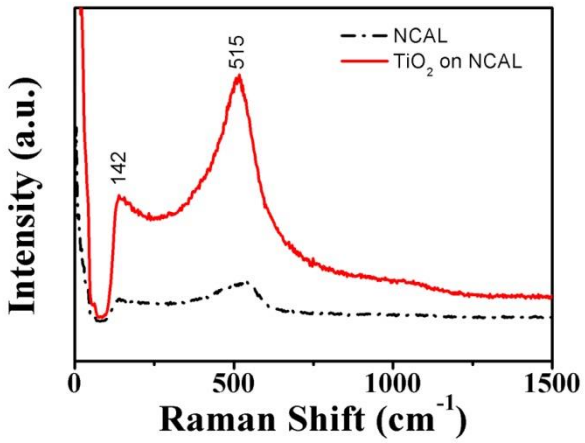


**Fig. S3** Raman spectra of NCAL and $TiO_2$ on NCAL.

Raman spectra were detected by NT-MDT (Russia) Raman spectrometer with 532 nm solid state laser at room temperature. The laser power on the sample was 20 mW. The Raman peaks 142, 515 $cm^{-1}$ are related to anatase $TiO_2$ [1, 2]. The observation of $TiO_2$ peaks are influenced by the Raman peaks of NCAL substrate as it has a relatively high background peak in the range of 100-550 $cm^{-1}$.

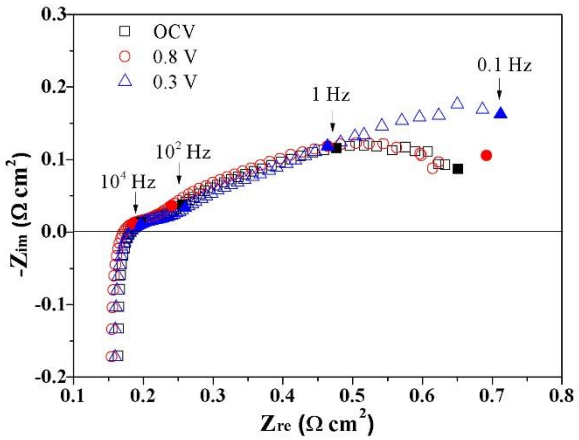


**Fig. S4** The electrochemical impedance spectra (EIS) of the cell at 550 °C under different voltage conditions.

EIS were taken under different voltage conditions: at 0.8 V, 0.3 V and at OCV for the cell. The

impedance is a little larger than that presented in Fig. 4b of the main paper because this fuel cell is not reverse operated.[3] From Fig. S4 we can see that the ohmic resistance (the intercept of the high frequency arc) was hardly affected by different voltage loads. The total polarization resistance, taken from the sum of high and low frequency arcs, gradually increased with the reduction of voltage from OCV to 0.3 V. Decreasing the cell voltage leads to the increasement of current and the enhancement of electrochemical reaction.[4] Accordingly, polarization resistance increases. The increase of low frequency semicircle, which can be assigned to mass transfer process, also indicates that the electrode polarization process, especially the gas diffusion process, is the rate limiting process.

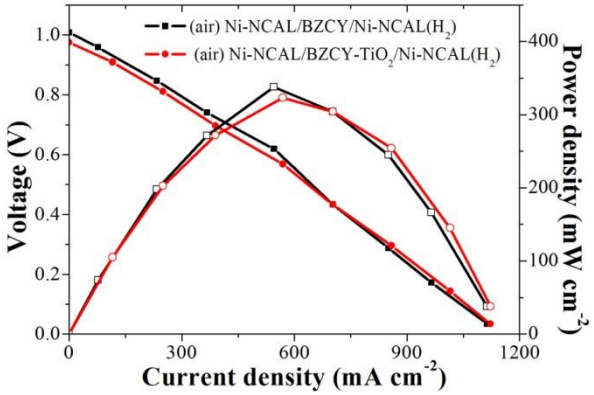


(a)

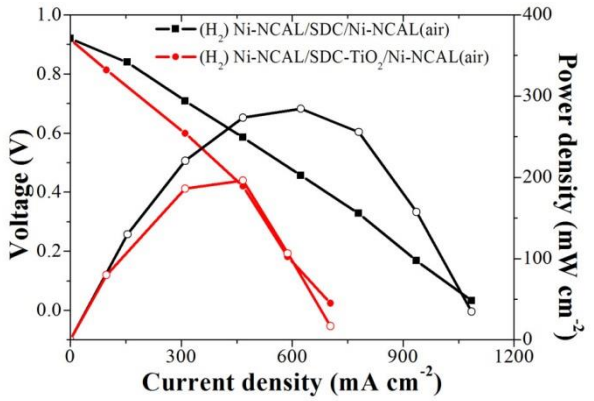


(b)

**Fig. S5** The I-V-P performance of fuel cells with and without blocking layer at 550 ºC.

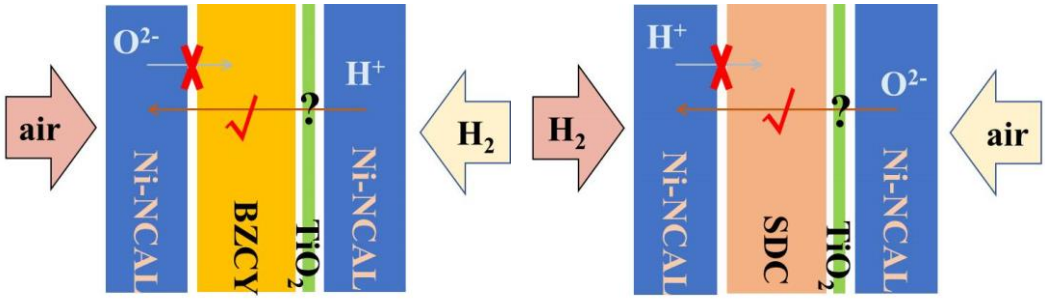


(a) (b)

**Fig. S6** Schematics of the fuel cell with BZCY as $O^{2-}$ blocking layer, and SDC as $H^{+}$ blocking layer.

The fabrication process of the cells is as follows. Firstly, 0.3 g SDC and BZCY were pressed into a pellet with 13 mm diameter, respectively. Then the pellets were annealed at 1000 ºC for 10 h. After cooling down, a solution of titanium diisopropoxide bis(acetylacetonate) (in 75% isopropanol, HeptaChroma) (TDB) that diluted in ethanol (1:3, volume ratio), was spin-coated on the SDC and BZCY pellets. The coating process was repeated for 10 times, followed by annealing at 500 ºC for 0.5 h to form $TiO_2$ film. Meanwhile, Ni foam pasted with NCAL powders was then dry-pressed into a pellet (Ni-NCAL). Finally, the $TiO_2$ coated SDC (or BZCY) pellet was sandwiched into two pieces of Ni-NCAL, forming a structure of Ni-NCAL/ SDC (BZCY)-$TiO_2$/ Ni-NCAL. In comparison, cell with structure Ni-NCAL/ SDC (BZCY) / Ni-NCAL was also studied. During the test, $H_2$ was supplied to cell Ni-NCAL/ SDC -$TiO_2$/ Ni-NCAL from the SDC side and air was supplied from the $TiO_2$ side, while for Ni-NCAL/ BZCY-$TiO_2$/ Ni-NCAL, $H_2$ was supplied from the $TiO_2$ side and air was applied from the BZCY side (Fig. S6).

From Fig. S5a, when using BZCY as the oxygen blocking layer, the two cells have similar performance, which are comparable with the performance of $TiO_2$ thin film electrolyte fuel cell in Fig. 4a of the main paper, indicating $TiO_2$ has proton conductivity. In Fig. S5b the maximum power density of cell Ni-NCAL/ SDC / Ni-NCAL is much higher than cell Ni-NCAL/ SDC -$TiO_2$/ Ni-NCAL,

indicating $TiO_2$ has rather poor $O^{2-}$ conductivity.

The structure of the above cells are presented in Fig. S6. It is notable that the $TiO_2$ thin films in these cells were not fabricated on NCAL substrate. For the cell Ni-NCAL/ BZCY-$TiO_2$/ Ni-NCAL, as the $TiO_2$ are facing the anode Ni-NCAL, protons that generated from $H_2$ by the catalyzation of NCAL, can still be intercalated into $TiO_2$. Whereas, for cell Ni-NCAL/ SDC-$TiO_2$/ Ni-NCAL, protons are blocked by SDC, so no protons can be transported through $TiO_2$, and the poor performance are resulted from its low oxygen ion conductivity.

## Reference


1. J. Zhang, M. Li, Z. Feng, J. Chen and C. Li, *J. Phys. Chem. B*, 2006, **110**, 927-935.
2. D. Praveen Kumar, N. Lakshmana Reddy, B. Srinivas, V. Durgakumari, V. Roddatis, O. Bondarchuk, M. Karthik, Y. Ikuma and M. V. Shankar, *Sol. Energy Mater. Sol. Cells*, 2016, **146**, 63-71.
3. X. Liu, W. Dong, Y. Tong, L. Wei, M. Yuan, X. Wang, B. Wang and B. Zhu, *Electrochim. Acta*, 2019, **295**, 325-332.
4. H. Ding, Y. Xie and X. Xue, *J. Power Sources*, 2011, **196**, 2602-2607.